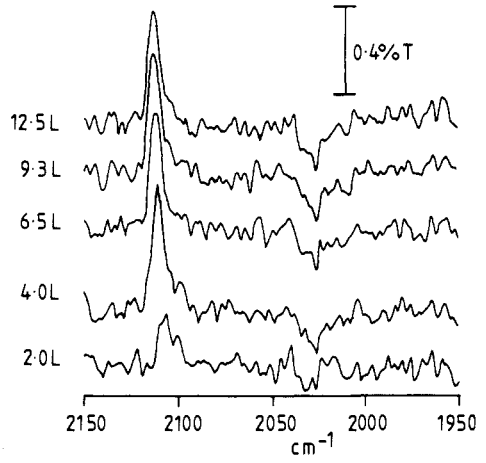

Figure 1. FT-RAIRS spectra of $Rh(CO)_2$ on $TiO_2(110)$ as a function of $[Rh(CO)_2Cl]_2$ exposure.

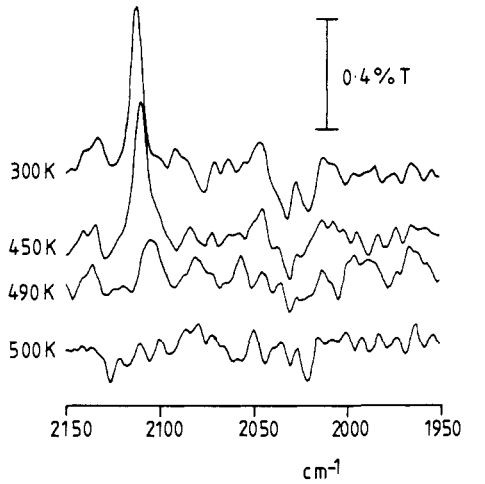

Figure 2. FT-RAIRS spectra of $Rh(CO)_2$ on $TiO_2(110)$ as a function of temperature.

to develop at 2112 cm^{-1} (p) together with a band at 2028 cm^{-1} (s), and they are assigned to the symmetric and antisymmetric $\nu(CO)$ vibrations of $Rh(CO)_2$. These values are close to those observed for this species on high area alumina,[3-16] silica,[6,16-18] and titania[6,16,17,19,20] surfaces. The reaction which leads to the *gem*-dicarbonyl involves the dissociation of the dimer and adsorption of chlorine on the TiO_2 surface.

The *gem*-dicarbonyl is stable on the $TiO_2(110)$ surface (in the presence of the chlorine generated by reaction of $[Rh(CO)_2Cl]_2$) to a temperature of 450 K. This is demonstrated in the series of FT-RAIRS spectra shown in Figure 2. These spectra have been obtained by heating the surface to successively higher temperatures, cooling to 300 K, and re-recording the IR spectrum. The peaks associated with the *gem*-dicarbonyl start to reduce in intensity by 450 K and have disappeared at 500 K. We have been able to study, using FT-RAIRS, the reversible CO adsorption on rhodium layers formed following this heat treatment. The $Rh(CO)_2$ species can be regenerated from the small islands or particles of metallic rhodium by the adsorption of CO at 1×10^{-3} Torr at 300 K. This is evidenced by the reappearance of the $\nu(CO)$ doublet (Figures 1 and 2) in the FT-RAIRS.

Acknowledgment. This work has been supported by the SERC (GR/F/52408), the University of Southampton, B.P. Research International, and B.P. Chemicals Ltd. We also acknowledge technical support from Perkin Elmer Ltd. and N. A. Williams for the preparation of $[Rh(CO)_2Cl]_2$.

(40) Patel, H.; Pemble, M. E. *J. Phys. IV* **1991**, *1*, 167.

Solution Conformation of a G·TA Triple in an Intramolecular Pyrimidine·Purine·Pyrimidine DNA Triplex

Ishwar Radhakrishnan[†] and Dinshaw J. Patel*[,†,‡]

Department of Biochemistry and Molecular Biophysics
College of Physicians and Surgeons
Columbia University
New York, New York 10032
Program in Cellular Biochemistry and Biophysics
Rockefeller Research Laboratories
Memorial Sloan-Kettering Cancer Center
New York, New York 10021

James M. Veal and Xiaolian Gao

Department of Structural and Biophysical Chemistry
Glaxo Inc. Research Institute
Research Triangle Park, North Carolina 27709

Received May 13, 1992

The DNA triple helix is a novel structural motif first discovered in homopurine·homopyrimidine polyribonucleotide sequences where the third pyrimidine strand binds in parallel with the purine strand in the major groove.[1,2] The recognition is achieved through sequence-specific hydrogen bonds formed between protonated cytidines and guanines or thymines and adenines leading to isomorphous C^+·GC and T·AT triples. Recently, stimulated by the potential application of triple helices in gene regulation, the scope of the triplex code has been extended to include G·TA[3] and T·CG[4] triples within the pyrimidine·purine·pyrimidine (Y·RY) triplexes. Although a structural model was proposed for the Y·RY motif based on an analysis of X-ray fiber-diffraction data nearly two decades ago,[5] no single-crystal or solution structure of any triplex has been reported.

We have determined the first three-dimensional solution structure of an intramolecular Y·RY triple helix **1**,[6] which contains a central purine·pyrimidine·purine G·TA triple flanked by canonical pyrimidine·purine·pyrimidine T·AT triples. In this report, the conformation of the G·TA triple in **1** will be discussed in detail as it is the only known instance in oligonucleotide-directed DNA recognition where a purine base recognizes a pyrimidine in a parallel orientation.[3] The structure elucidation was based on experimental NMR data[7] which provided torsion angle and proton–proton distance estimates. Our previous work, especially, established the presence of a number of interstrand contacts involving the third strand which were important in defining the

[†] Columbia University.
[‡] Memorial Sloan-Kettering Cancer Center.

(1) Felsenfeld, G.; Davies, D.; Rich, A. *J. Am. Chem. Soc.* **1957**, *79*, 2023-2024.
(2) (a) Reviewed: Wells, R. D.; Collier, D. A.; Hanvey, J. C.; Shimizu, M.; Wohlraub, F. *FASEB J.* **1988**, *2*, 2939-2949 (and references cited therein). (b) Moser, H.; Dervan, P. B. *Science* **1987**, *238*, 645-650. (c) Le Doan, T.; Perronault, L.; Praseuth, D.; Habhoub, N.; Decout, J. L.; Thuong, N. T.; Lhomme, J.; Helene, C. *Nucl. Acids Res.* **1987**, *15*, 7749-7760. (d) de los Santos, C.; Rosen, M.; Patel, D. *Biochemistry* **1989**, *28*, 7282-7288. (e) Rajagopal, P.; Feigon, J. *Biochemistry* **1989**, *28*, 7859-7870. (f) Plum, G. E.; Park, Y. W.; Singleton, S. F.; Dervan, P. B.; Breslauer, K. J. *Proc. Natl. Acad. Sci. U.S.A.* **1990**, *87*, 9436-9440. (g) Roberts, R. W.; Crothers, D. M. *Proc. Natl. Acad. Sci. U.S.A.* **1991**, *88*, 9397-9401.
(3) (a) Griffin, L. C.; Dervan, P. B. *Science* **1989**, *245*, 967-971. (b) Kiessling, L. L.; Griffin, L. C.; Dervan, P. B. *Biochemistry* **1992**, *31*, 2829-2834.
(4) Yoon, K.; Hobbs, C. A.; Koch, J.; Sardaro, M.; Kutny, R.; Weis, A. L. *Proc. Natl. Acad. Sci. U.S.A.* **1992**, *89*, 3840-3844.
(5) (a) Arnott, S.; Selsing, E. *J. Mol. Biol.* **1974**, *88*, 509-521. (b) Arnott, S.; Bond, P. J.; Selsing, E.; Smith, P. J. C. *Nucl. Acids Res.* **1976**, *3*, 2459-2470.
(6) Intramolecular Y·RY triplexes where the stems are linked by pyrimidine loops have been proposed: (a) Haner, R.; Dervan, P. B. *Biochemistry* **1990**, *29*, 9761-9765. (b) Sklenar, V.; Feigon, J. *Nature* **1990**, *345*, 836-838. (c) Radhakrishnan, I.; Patel, D. J.; Gao, X. *J. Am. Chem. Soc.* **1991**, *113*, 8542-8544.
(7) (a) Radhakrishnan, I.; Gao, X.; de los Santos, C.; Live, D.; Patel, D. J. *Biochemistry* **1991**, *30*, 9022-9030. (b) Radhakrishnan, I.; Patel, D. J.; Gao, X. *Biochemistry* **1992**, *31*, 2514-2523.

0002-7863/92/1514-6913$03.00/0

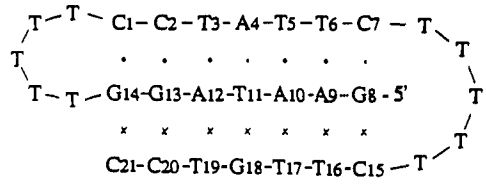

1

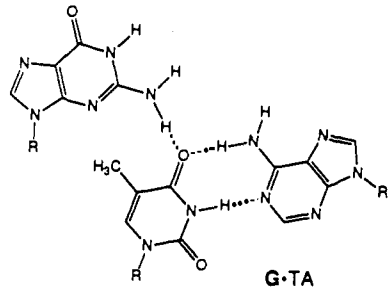

2

orientation of this strand relative to the duplex.[7] Restrained molecular dynamic simulations[8] in the presence of explicit solvent and sodium counterions were undertaken on the seven base triple segment of triplex **1** with the hairpin loops excluded due to the lack of detailed experimental information in these regions. Six refined structures were obtained (pairwise average RMSD of 1.20 ± 0.42 Å) from two starting structures using three different seeds for initial velocity assignments.[9]

Analysis of a representative structure designated TRIX-I using the CURVES program[11] for the Watson–Crick duplex within the triple helix revealed that despite the interruption of a homopurine·homopyrimidine tract by a pyrimidine·purine base pair, the overall axial rise, helical twist, and base-pair inclination are very similar to those in the fiber-diffraction model.[12] In both structures the base pairs are displaced from the helical axis, although the displacement in the solution structure is much less.[12]

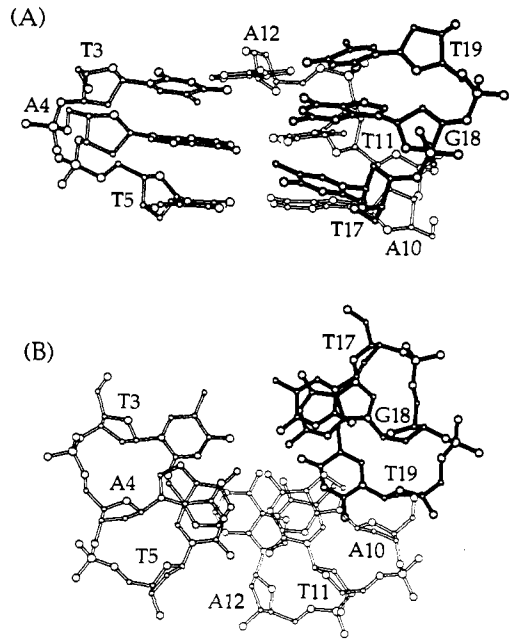

Figure 1. The TRIX-I refined structure of the (T17-G18-T19)·(A10-T11-A12)·(T3-A4-T5) central segment of the intramolecular triplex **1**. (A) This view is normal to the helical axis and looks into the major groove of the Watson–Crick duplex segment of the triplex. G18, T11 and A4 constitute the G·TA triple. (B) This view is down the helical axis with the T17-G18-T19 third strand closer to the A10-T11-A12 purine strand. Note that G18 stacks over T17 but not over T19.

In contrast, while the fiber-diffraction model[5] assumed an N-type conformation for the sugars, with the exception of G18, the majority of these moieties in the solution structures display a propensity toward an S-type conformation. The few sugars which possess more N-type character belong to pyrimidine residues in agreement with other recent studies.[13,14] The third strand is in a closer disposition to the purine strand with which it forms Hoogsteen base pairs on triplex formation. The helical twist (~31°) results in an underwound DNA relative to the canonical A- and B-forms.

The central G·TA triple and its flanking T·AT triples are well-defined in the superpositioned refined structures shown in the supplementary Figure 1 (average pairwise RMSD 0.83 ± 0.19 Å). The guanine base is oriented such that the Hoogsteen edge is exposed to the solvent, while the Watson–Crick edge is buried in the major groove. The TA base pair in the G·TA triple retains Watson–Crick hydrogen bonds, and there is no indication of any significant perturbations at this site. We can identify which of the two amino protons of G18 is hydrogen bonded to the O^4 carbonyl of T11 within the G·TA triple as shown schematically in **2**. The presence of the purine G18 in an otherwise homopyrimidine segment necessitates local structural readjustments. The guanine is tilted out of plane of the TA base pair it recognizes, toward its 3′-direction (Figure 1A), and this effect is transmitted to its 5′ neighboring base T17. In this orientation, an additional hydrogen bonding interaction,[15] albeit weak, can be identified between the other guanine amino proton and the O^4 carbonyl of T3 belonging to the *adjacent* T·AT triple. Further, the guanine is rotated away relative to the center of the helix presumably, to avoid a steric clash with the methyl group of T11 within the same triple. Consequently, G18 stacks well with the 5′-linked base T17

(8) (a) A total of 492 distances and 13 torsion angles were restrained in the simulations conducted in the presence of explicit solvent and 15 Na^+ counterions using the X-PLOR program (Brunger, A. T.). Each simulation lasted a total of 6.3 ps which took approximately 180 min of CPU time on a CRAY Y-MP and consisted of a heating phase, followed by an equilibration phase before the force constants of the NMR-based restraints were scaled up to their final values at 400 K. The system was cooled to 300 K and equilibrated before being subjected to a final minimization. (b) The interproton distances from 2D NOESY data sets recorded in D_2O were calculated from buildup curves using the isolated spin-pair approximation, while those derived from a 2D NOESY (τ_m = 170 ms) spectrum recorded in H_2O and a 3D NOESY–TOCSY (τ_m = 200 ms) spectrum recorded in D_2O were computed directly by comparing the NOE cross-peak intensities with a suitable reference. Further, these distances were supplemented by hydrogen-bonding restraints between base pairs (except between G18 and T11 in the G·TA triple) as well as "repulsive" restraints between selected proton pairs that do not show NOEs. The bounds for the restraints from the 2D data set collected in D_2O were specified as follows: For distances (d_{ij}) less than 3.0 Å, −0.2 Å/+0.3 Å, for 3.0 Å < d_{ij} < 4.0 Å, −0.3 Å/+0.4 Å, and for d_{ij} > 4.0 Å, ±0.4 Å. The distances involving methyl protons were relaxed by 0.5 Å, while diffusion-prone proton pairs were given suitable wider upper bounds. The error estimates for exchangeable protons were set at ±10% of their target values to account for their lower occupancy numbers and contributions from spin-diffusion which is usually not severe in these cases. Distances derived from the 3D data set were restrained to less than 5.5 Å. Relaxation matrix refinement of the structures are currently being undertaken to bring the structures closer in agreement with the experimental data.

(9) The starting structures were constructed from the fiber-diffraction model[5] or from the parameters for B-form DNA[10] (RMSD 3.35 Å before dynamics). The final structures obtained from each of the two starting structures were very similar relative to one another except in regions that were underdetermined due to a lack of NMR constraints. These regions include residues T6 and C7 at the 3′-end of the first strand and residue A12 in the purine strand. In the case of the former, the structures bear the characteristics of their starting structures.

(10) Arnott, S.; Hukins, D. W. L. *J. Mol. Biol.* **1973**, *81*, 93–105.

(11) (a) Lavery, R.; Sklenar, H. *J. Biomol. Str. Dyn.* **1988**, *6*, 63–91. (b) Lavery, R.; Sklenar, H. *J. Biomol. Str. Dyn.* **1989**, *6*, 655–667.

(12) Average values for some of the helical parameters observed in the fiber-diffraction model[5] and in our structure are as follows: (a) axial rise (Å) 3.26, 3.44; (b) helical twist (deg) 30.0, 31.0; (c) inclination (deg) 3.8, −0.5; and (d) X-displacement (Å) 3.55, 2.08, respectively.

(13) Laughton, C. A.; Neidle, S. *J. Mol. Biol.* **1992**, *223*, 519–529.

(14) Macaya, R. F.; Schultze, P.; Feigon, J. *J. Am. Chem. Soc.* **1992**, *114*, 781–783.

(15) The observed ranges in our structures for this interaction are as follows: r_{A-H} = 2.71 ± 0.2 Å and $\angle_{D-H-A}$ = 168 ± 8°, where A and D denote the heavy atom acceptor and donor, respectively.

and poorly with the 3′-linked base T19 (Figure 1B). More interestingly, unlike the other residues in the triplex, the guanine sugar adopts a typical N-type conformation (C2′-exo). Stereopairs of Figure 1 are included separately as supplementary Figure 2.

In summary, using experimental NMR restraints and molecular dynamics, we have demonstrated the structural features unique to the G·TA triple **2** in an intramolecular Y·RY DNA triplex **1** in solution. The accommodation of the purine base in a homopyrimidine third strand can be attributed to the readjustments in the local structure of the G18 purine base and sugar pucker and an unusual base stacking interaction. One guanine amino proton hydrogen bonds with the thymine carbonyl within the G·TA triple, while the other guanine amino proton weakly hydrogen bonds with the thymine carbonyl of the adjacent T·AT triple. This demonstration that the third strand guanine recognizes local structural features defined by adjacent residues was anticipated in earlier contributions from Dervan's[3b] and Helene's[16] laboratories.

Acknowledgment. We thank Dr. Charles Laughton for helpful discussions. This work was supported, in part, by an NIH Grant GM-34504 to D.J.P. The Molecular Modeling Facility for Molecular Biology at Columbia University was supported under NSF Grant DIR-8720229. The access to the Cray Y-MP Supercomputer at North Carolina provided by Glaxo Inc. Research Institute is gratefully acknowledged.

Supplementary Material Available: Stereoviews of a superposition of six refined structures of the (T17-G18-T19)·(A10-T11-A12)·(T3-A4-T5) central segment of triplex **1** (3 pages). Ordering information is given on any current masthead page.

(16) Mergny, J. L.; Sun, J. S.; Rougee, M.; Montenay-Garestier, T.; Barcelo, F.; Chomilier, J.; Helene, C. *Biochemistry* **1991**, *30*, 9791–9798.

A New Synthesis of Methano-Bridged Annulenes: Access to Highly Substituted Derivatives

David G. Barrett, Gui-Bai Liang, and Samuel H. Gellman*

S. M. McElvain Laboratory of Organic Chemistry
Department of Chemistry, University of Wisconsin
1101 University Avenue, Madison, Wisconsin 53706

Received February 4, 1992

The synthesis of 1,6-methanol[10]annulene (**1**) was first reported by Vogel and Roth in 1964,[1] and many aspects of the chemistry of the methano-bridged annulenes have been elucidated by the laboratories of Vogel,[2,3] Paquette,[4] and others in the intervening years. We became interested in derivatives of **1** bearing

1

polar substituents on the methylene bridge because of their unusual amphiphilic topology: one face of the rigid structure is nonpolar, and the other face is polar. Incorporation of such double-sided amphiphilic subunits into larger structures should lead to molecules with interesting complexation and/or aggregation properties.[5] In order to employ bridged annulenes as architectural elements in larger structures, however, one requires derivatives bearing functionality on both the methylene bridge and the aromatic platform; no examples of this type of doubly functionalized bridged annulene have been previously reported, to our knowledge. We describe a new synthetic approach to the 1,6-methano[10]annulene framework that provides efficient access to highly substituted derivatives.

Scheme I[a]

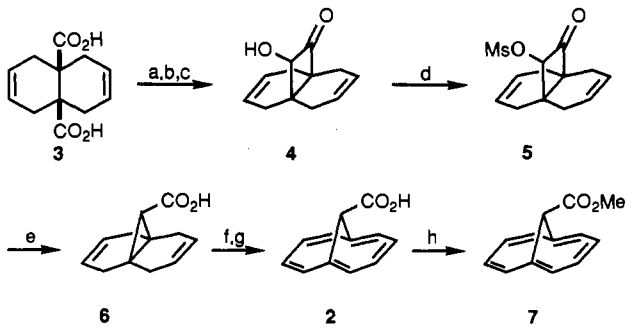

[a] Key: (a) $(MeO)_2SO_2$, K_2CO_3, MeCN; (b) Na, K, Me_3SiCl, Et_2O; (c) MeOH; (d) MsCl, Et_3N, CH_2Cl_2; (e) LiOH, THF, H_2O; (f) Br_2, CH_2Cl_2; (g) *t*-BuOK, THF; (h) $(MeO)_2SO_2$, K_2CO_3, MeCN.

Scheme II[a]

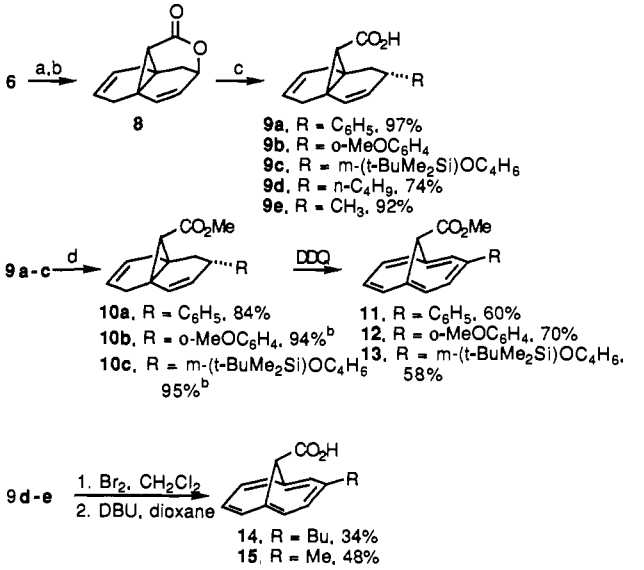

[a] Key: (a) I_2, KI, $NaHCO_3$, H_2O; (b) DBU, benzene; (c) cuprate;[9] (d) $(MeO)_2SO_2$, K_2CO_3, MeCN. [b] Yields from **8**.

The merits of the new route are illustrated by the synthesis of acid **2**[3,4] shown in Scheme I. Dicarboxylic acid **3**[6] was converted in three steps (92% overall yield) to propellane **4**,[7,8] which could then be converted quantitatively to the mesylate. The key transformation was a LiOH-induced semi-benzylic Favorskii rearrangement[9] of **5** that produced **6** in 96% yield (the overall yield of **6** from **3** was 88%). The previously reported synthesis of **6** proceeds in three steps and 13% overall yield from isotetralin in a route that requires several chromatographic separations;[4] our synthesis of **6** proceeds in superior yield and requires chromatography of only mesylate **5**. Treatment of **6** with Br_2 yielded a mixture of stereoisomeric tribromo lactones which, when allowed to react with *t*-BuOK, produced annulene **2** in 95% yield (from **6**). Formation of ester **7** from **2** and $(MeO)_2SO_2/K_2CO_3$ was quantitative under standard conditions. Acid **6** has previously

(1) Vogel, E.; Roth, H. D. *Angew. Chem.* **1964**, *76*, 145.
(2) Vogel, E. *Chimia* **1968**, *22*, 21.
(3) Vogel, E. *Spec. Publ.—Chem. Soc.* **1967**, No. 21, 113.
(4) Paquette, L.; Heyd, W. E.; Thompson, G. L. *J. Am. Chem. Soc.* **1974**, *96*, 3177.
(5) For a recent study of a family of amphiphiles containing a subunit with a related double-sided amphiphilic topology, and a general discussion of amphiphile topology, see: Stein, T. M.; Gellman, S. H. *J. Am. Chem. Soc.* **1992**, *114*, 3943.
(6) Spur, P. R.; Hamon, D. P. G. *J. Am. Chem. Soc.* **1983**, *105*, 4734.
(7) Propellane **4** has previously been prepared in three steps and 45–55% overall yield from the anhydride of **3**: Bloomfield, J. J.; Irelan, J. R. S. *J. Org. Chem.* **1966**, *31*, 2017 and references therein.
(8) In situ trapping of acyloin condensation products with trimethylsilyl chloride: Bloomfield, J. J.; Melke, J. M. *Org. Synth.* **1977**, *57*, 1.
(9) Kirmse, W.; Olbricht, T. *Synthesis* **1975**, 173.

0002-7863/92/1514-6915$03.00/0